

Combined Analytical Py-GC-MS, SEM, FTIR and ¹³C NMR for Investigating the Removal of Trace Metals from Aqueous Solutions by Biochar

Minéia A. M. de Andrade,^a Adnivia S. C. Monteiro,^b Erik S. J. Gontijo,^{b,a}
Carolina C. Bueno,^{a,c} João C. A. Macedo,^a Elidiane C. Rangel,^a Darllene S. Melo,^a
José I. Z. Montero^a and André H. Rosa^{b,*a}

^aInstituto de Ciência e Tecnologia (ICT), Universidade Estadual Paulista (Unesp),
Av. Três de Março, 511, Alto da Boa Vista, 18087-180 Sorocaba-SP, Brazil

^bPrograma de Pós-Graduação em Recursos Hídricos (PRORH), Universidade Federal de Sergipe (UFS),
Av. Marechal Rondon, s/n, Jd. Rosa Elze, 49100-000 São Cristovão-SE, Brazil

^cDepartment of Geography and Geosciences, GeoZentrum Nordbayern,
Friedrich-Alexander University Erlangen-Nürnberg (FAU), Universitätsstraße 40, 91054 Erlangen, Germany

In this study, the efficiency of biochar (BC) produced from sugarcane bagasse at different pyrolysis temperatures (300, 400, 500 and 600 °C) for simultaneous removal of Cd^{II}, Pb^{II}, Cu^{II}, Cr^{III}, Ni^{II} and Zn^{II} ions from aqueous solutions was assessed. All BC were characterized using scanning electron microscopy (SEM), Fourier transform infrared (FTIR), ¹³C nuclear magnetic resonance (¹³C NMR) and pyrolysis-gas chromatography-mass spectrometry (Py-GC-MS). The effects of pyrolysis temperature, initial adsorbate concentration and adsorbent dosage on adsorption capacity of BC were examined through batch experiments. The BC efficiency was also evaluated after a desorption cycle. The maximal adsorptions (Cd^{II}: 51.50%, Cr^{III}: 74.35%, Cu^{II}: 91.18%, Ni^{II}: 47.05%, Pb^{II}: 96.17% and Zn^{II}: 40.50%) were observed for BC produced at 500 °C, probably because of its higher porosity and presence of functional groups detected by SEM and FTIR. The maximum adsorption capacity for Cd^{II}, Cr^{III}, Cu^{II}, Ni^{II} and Zn^{II} (ions fitted to Langmuir model) were 175, 303, 455, 156 and 128 µg g⁻¹, respectively. The predominance of phenolic groups observed in Py-GC-MS data may explain the high percentage of multi-element removal. Experimental data were best fitted to pseudo-second order, Sips and Freundlich models. The BC presented good removal results after a desorption cycle.

Keywords: low-cost adsorbents, adsorption, heavy metals, multi-element solution, isotherms

Introduction

Trace metals such as Cd, Cr, Cu, Ni, Pb and Zn are classified as significant water pollutants due to their persistence, high toxicity and tendency of bioaccumulation.¹ Although they occur naturally in rocks (geogenic sources), most of contamination sources and human exposure are derived from anthropogenic activities, including agriculture, battery, mining, textile and tanning industries.²⁻⁴ The rapid industrialization and urbanization are increasing the levels of these chemicals in environment, raising concerns over the impacts of these pollutants on ecosystems and human health. All these factors are also contributing to potable water scarcity, requiring the development of cheap and

efficient techniques to simultaneously remove all dangerous chemicals from natural waters and effluents.⁵

The methods conventionally used to remove trace metals from aqueous solutions are chemical precipitation (e.g., hydroxide precipitation and sulfide precipitation), ion exchange and adsorption methods. The chemical precipitation is the most used from these methods for treatment in industry. It consists basically in a reaction between chemicals and trace metals producing insoluble precipitates, which can be removed via sedimentation or filtration.⁶ Ion exchange methods are known to have fast kinetics and high treatment capacity,⁷ involving for instance the use of a strong acid cation-exchanger (synthetic or natural solid resin) that removes the contaminants from water.^{6,7} Adsorption is a process that offers flexibility in the treatment and sometimes can be reversible, consisting

*e-mail: andre.rosa@unesp.br

in the accumulation of contaminants at the interface of two phases. The sorption can be physical (via van der Waals forces) or chemical (chemical bonding).^{6,8}

Among all adsorption methods, biosorption is the most cost effective and environmentally friendly technique since it can provide a high trace metal removal efficiency and reduce the amounts of residues produced by agriculture.⁹ These residues include bagasse from crops, non-living biomass (bark, lignin, shrimp, krill, etc.) and algal or microbial biomass.⁶

A biosorbent largely used for treatment of contaminated waters with trace metals is biochar (BC), which is a carbon-rich material derived from the thermal decomposition of organic matter in low oxygen content atmosphere. It can be produced from a large range of feedstocks at different pyrolysis conditions that can change its adsorption characteristics and removal efficiency.¹⁰ Furthermore, the presence of micro and/or mesoporous, surface functional groups (carboxyl, carbonyl, hydroxyl, among other groups) in its structure gives the BC a promising potential in removing trace metal ions from water systems. Despite this, very little is known about the removal efficiency of multiple trace metal ions coexisting in aqueous solutions (competitive adsorption) by BC from different materials, as pointed out by Park *et al.*¹¹ These authors reported that Cd lost most of its adsorption capacity on BC of sesame straw under multielement (Cd, Cr, Cu, Pb and Zn) conditions. These ions can occur simultaneously in both natural waters and effluents (e.g., from textile dyeing industry), supporting this kind of investigation.¹²

Biochars produced from residues of local crops can be used as alternative adsorbent for trace metals removal. The BC used in this work was made from sugarcane bagasse (SB) since it is an important by-product of sugar production in the world and there is a great need to find a valuable destination for this type of waste. Brazil is the largest sugarcane producer country in the world, with a production of 652 million tons in the 2016/2017 harvest.¹³ This fact by itself demonstrates the great potential of the amount of agricultural residues production of the sugar industry. Among these residues, SB is one of the by-products created in massive volumes from sugar and alcohol industries.¹⁴ Nearly 123 million tons of sugarcane are produced every year in China, and about 5.2 million tons of sugarcane bagasse are generated annually.¹⁵ According to Saadati and Hosseinezhad,¹⁶ one of the problems of the sugar industry is the management of the large amount of produced bagasse, which sometimes exceed 2 Tg *per* year just in one sugar mill located in Iran, for instance. The sugarcane bagasse represents 25 to 30% of the product's weight and nearly 65 to 75% of the SB produced in the farms, mills and industry is burned into boilers for steam

and power generation.^{17,18} Nevertheless, this method may not be suitable in organic waste management due to pollutant emissions, economic and labor costs, loss of energy, and bad odour.¹⁹ Because of that, the post-harvest residues in the industry can no longer be considered as the final product from a sugar mill or first-generation ethanol fabrication and requires a long-term innovation to ensure the environmental quality and profitability of sugarcane crops.²⁰ The sugarcane bagasse residues are not only of critical importance to Brazil sugar industry, but also to South Africa, the United States, Australia, India, and China which maintain an increasing demand for sugarcane feedstock for the sugar industry and also to expand bioethanol production.²¹

In addition, the SB is proven to be a great raw material for the production of BC, since vegetal based-BC has its original structures, such as cellulose, hemicellulose, and lignin, which maintain functional groups such as carboxylic acids, alcohols, and amines with high affinity for metal ions.²²⁻²⁴ It is also important to highlight that BC made of SB is an environmental friendly product since sugarcane crops grows faster than trees (wood is used to produce activated carbon), which means that the use of this raw material for biosorbent production helps to reduce our dependence on harvesting trees.

The aim of this study was to evaluate the adsorption capacity of BC from SB in removing simultaneously the potentially toxic trace metals Cd^{II}, Cr^{III}, Cu^{II}, Ni^{II}, Pb^{II} and Zn^{II} from aqueous solutions. Several analytical techniques (pyrolysis-gas chromatography-mass spectrometry (Py-GC-MS), scanning electron microscopy (SEM), Fourier transform infrared (FTIR), ¹³C nuclear magnetic resonance (¹³C NMR)) were used for characterizing BC and understanding the simultaneous removal of the trace metals. Furthermore, the desorption capabilities of this material were assessed in order to evaluate the use of BC from SB as filter for removal of the mentioned metals from multielement aqueous solutions. A range of experiments were performed using different pH conditions and BC produced at different pyrolysis temperatures. Since the BC used in this study was produced from SB, this research would contribute to add commercial value to leftovers from sugarcane crops. Moreover, the utilization of BC would reduce the impacts caused by poor management of residues of sugarcane crops, especially for big producers worldwide.

Experimental

Biochar preparation

Sugarcane bagasse was used to produce raw and modified BC. The biomass was firstly washed with tap

water and dried in drying oven at 80 °C for 24 h. The dried biomass was crushed (Willey mill MA048 at 1730 rpm) and then pyrolyzed (60 g) using cylindrical reactor (0.82 cm³) using a muffle oven at different temperatures regimes (300, 400, 500 and 600 °C, named BC300, BC400, BC500 and BC600, respectively) at a rate of 5 °C min⁻¹ (slow pyrolysis). The target temperature was kept for 2 h in a low-oxygen environment. Subsequently the sugarcane biochars (BC-SC) were cooled at room temperature overnight, sieved (35-mesh sieve) and stored in polypropylene bottles until analysis.

Pyrolysis coupled to gas chromatography with mass spectrometry (Py-GC-MS)

The biomass and BC produced were characterized using Py-GC-MS. The technique provides a high level of structural information of the materials analyzed in a fast and inexpensive way, although some limitation related to the semi-quantitative nature of the technique.²⁵ The analyses were carried out using a Varian 450-GC Gas Chromatograph (with a HP-5 column: 30 m-long × 0.25 mm, 0.25 m) with a Varian Saturn 2000 ion-trap mass spectrometer set at an electron ionization at 70 eV in full scan acquisition (*m/z* 10-450). A pyrolyzer (CDS 5000 Series Pyroprobe) was coupled to the mass spectrometer and the method used was described by Fabbri *et al.*²⁶

^{13}C nuclear magnetic resonance (^{13}C NMR)

^{13}C NMR analyses were conducted on a Bruker spectrometer (Avance III 400 MHz WB model) operating at 50.3 MHz frequency. Samples (approximately 100 mg of BC300, BC400, BC500 and BC600) were packed in a 4 mm rotor and then analyzed under the following experimental conditions: band spectral cross-polarization, magic-angle spinning, 5.5 kHz, 4 μs proton preparation pulse, a contact time of 2 ms, acquisition time of 20 ms, and wait time for relaxation of 5 s. Chemical shifts were expressed in ppm. Data were analyzed using the ACD/NMR software Processor Academic Edition.²⁷ The plots of the groups of carbon present in the samples were obtained by integrating the peaks present in the spectra according to the methodology described by Stevenson.²⁷

Scanning electron microscopy (SEM)

Surface morphology and pore diameter were evaluated by means of SEM (JEOL JSM-6010LA). The BC samples were coated with Au/Pd thin conductive coating (via sputtering) before analysis to avoid charging effects during

the inspections. Secondary electron micrographs were taken with amplification of 5 to 200 μm, using beam energy of 5 keV, spot size of 30 and working distance of 16 mm from the most representative region of the samples.

Fourier transform infrared spectroscopy (FTIR)

FTIR spectra were taken to identify the functional groups of all different BC produced and their interactions with trace metals. The spectra, recorded with 4 cm⁻¹ resolution in the spectral range between 4000 and 650 cm⁻¹ (32 scans), were collected using a Fourier transform infrared spectrometer (PerkinElmer® Spectrum 65 FTIR) in the attenuated total reflection (ATR).

Adsorption of trace metals by biochars produced at different pyrolysis temperatures

The experiments were carried out adding BC (0.2 g) produced at different pyrolysis temperatures (BC300, BC400, BC500 and BC600) in 100 mL (500 μg L⁻¹) multielement solutions containing Cd^{II}, Cr^{III}, Cu^{II}, Ni^{II}, Pb^{II} and Zn^{II}, which were prepared from dilutions of individual standard SpecSol® (1000 mg L⁻¹, Quimlab, Jacareí, Brazil). The samples were shaken at 175 rpm and aliquots were taken at specific times (0, 30, 60, 90, 180, 300, 360, 420, 480, 540, 600 and 1440 min). Afterwards, all trace metals were analyzed using an inductively coupled plasma optical emission spectroscopy (ICP OES). The removal rate for each BC was calculated from the time when the equilibrium was reached. Kinetic studies were performed using the BC with highest removal rate.

Influence of the initial concentration of trace metals on biochar removal

A preliminary evaluation of the best conditions to conduct experiments with BC was carried out adding 0.2 g of BC in 100 mL multielement solutions containing different concentrations (100, 300, 500 and 700 μg L⁻¹) of Cd^{II}, Cr^{III}, Cu^{II}, Ni^{II}, Pb^{II} and Zn^{II}. The samples were shaken at 175 rpm in an incubator shaker for 1440 min at 25 °C for all tests. Aliquots were taken during specific times (0, 30, 60, 90, 180, 300, 360, 420, 480, 540, 600 and 1440 min) and subsequently filtrated through 0.45 μm membrane before metal determination.

Effect of adsorbent dose on adsorption

Different amounts (0.2, 0.3, 0.4 and 0.5 g) of the BC with best removal efficiency were added in 100 mL solutions

containing Cu^{II}, Cd^{II}, Cr^{III}, Ni^{II}, Pb^{II} and Zn^{II}. The initial concentrations (500 µg L⁻¹) for all metals were determined in previous tests. The samples were shaken at 175 rpm in an incubator shaker at 25 °C and aliquots were taken at specific times and filtrated through 0.45 µm membrane filters. All experiments were performed in duplicate and the metal concentrations were determined using an ICP OES.

Adsorption kinetics

The adsorption kinetics on removal of Cu^{II}, Cd^{II}, Cr^{III}, Ni^{II}, Pb^{II} and Zn^{II} was studied by adding 0.2 g of BC in 100 mL of solution, using the best conditions found in previous experiments. The solutions were shaken at 25 °C in an incubator shaker and aliquots were taken at specific times and determined as described in previous "Adsorption of trace metals by biochars produced at different pyrolysis temperatures" sub-section. All trials were performed in duplicate.

Adsorption isotherms

Adsorption isotherms of Cu^{II}, Cd^{II}, Cr^{III}, Ni^{II}, Pb^{II} and Zn^{II} onto BC were determined by adding 0.2 g of BC500 in 100 mL of multielement solution in different concentrations (100, 200, 300, 400, 500, 600, 700 and 800 µg L⁻¹). The samples were shaken under the same conditions described in previous experiments. The samples were filtrated (0.45 µm membrane filters) and the metals determined through ICP OES.

Experiments with activated carbon

Galán *et al.*²⁸ state that activated carbon is the most widely used material in adsorption processes. However, according to Saka *et al.*,²⁹ this element presents a high acquisition cost and needs to be regenerated after each application. In this context, it was decided to compare the removal efficiency of the BC with the activated carbon.

Kinetic tests using activated carbon (Dinâmica, Indaiatuba, Brazil) were carried out using the same conditions of the BC-SC. In this way, 0.2 g of activated carbon was added in a 100 mL solution (500 µg L⁻¹) of Cu^{II}, Cd^{II}, Cr^{III}, Ni^{II}, Pb^{II} and Zn^{II}. The samples were shaken at 175 rpm in a shaker incubator during 1440 min at room temperature. Aliquots were taken after 10, 20, 30, 45, 60, 90, 180, 300, 360, 420, 480, 540, 600 and 1440 min and analyzed in an ICP OES.

The experiments described in past sections were performed at pH 5 based on previous experiments (Figure S2, Supplementary Information (SI) section) and

studies (such as Kołodyńska *et al.*³⁰ and Ding *et al.*)³¹ where the pH 5 had the maximum adsorption efficiency. At higher pHs, the sorption capacity values would decrease because the metal ions would start to hydrolyze and precipitate.³² The Cd and Pb for instance can precipitate at high pH solution (pH > 7 for Cd and pH > 5 for Pb) as stated by Ding *et al.*³³ Park *et al.*³⁴ indicated that the metal precipitation can be avoided at pH less than 7. On the other hand, the adsorption of some analyzed cations can be lower at low pH due to electrostatic repulsion between the BC surface and the cations.

Desorption and regeneration capacity of BC

The desorption experiments started with an adsorption cycle performed under similar conditions as described for the batch adsorption experiments (0.2 g of BC500, 100 mL of multielement solution (Cu^{II}, Cd^{II}, Cr^{III}, Ni^{II}, Pb^{II} and Zn^{II} at original concentration of 500 µg L⁻¹), pH 5 and 25 °C). After the adsorption cycle, the BC500 was dried, weighted and treated with 100 mL of HNO₃ (0.1 mol L⁻¹) solution during 10 h to evaluate the desorption percentage (D).³⁵ Afterwards, another adsorption was performed using the same conditions of the first adsorption in order to evaluate the BC500 regeneration capacity.

Theory/calculation

The amount of metals adsorbed on BC-SC (q , µg of metal *per* g of adsorbent) was determined through the following equation:³⁶

$$q = [(C_0 - C_f) \times V] / m \quad (1)$$

where C_0 and C_f are, respectively, the initial and final ion concentration of each metal in the solution (µg L⁻¹). The volume of solution (V) and adsorbent dose (g) are correspondingly V and m . The percentage of metal removal (Q) was calculated using the equation:

$$Q = [(C_0 - C_f) / C_0] \times 100 \quad (2)$$

Pseudo-first order and pseudo-second models were fit to the experimental data in order to clarify the adsorption reaction mechanisms and predict the speed of metal removal from the aqueous solutions.³⁷ The pseudo-first and -second order models were calculated according to equations 3 and 4, respectively:³⁷⁻³⁹

$$q_t = Q_e(1 - \exp(-K_1 t)) \quad (3)$$

$$q_t = (K_2(Q_e)^2 t) / (1 + Q_e K_2 t) \quad (4)$$

where, q_t is the metal adsorbed at a given time t ($\mu\text{g g}^{-1}$), Q_e is the amount adsorbed ($\mu\text{g g}^{-1}$) at equilibrium time (min), K_1 is the rate constant of pseudo-first order kinetics model (min^{-1}) and K_2 is the rate constant of pseudo-second order kinetics model ($\mu\text{g (g min}^{-1}\text{)}^{-1}$).

The mechanism of the adsorption process was evaluated by the Langmuir (that assumes monolayer and homogeneous adsorption) and Freundlich (that assumes multilayer adsorption) isotherms, being described by equations 5 and 6:⁴⁰⁻⁴²

$$Q_e = (q_{\text{max}}K_L C_e) / (1 + K_L C_e) \quad (5)$$

$$Q_e = N_F C_e^{1/n} \quad (6)$$

where Q_e is the amount of trace metal adsorbed *per* weight of biochar ($\mu\text{g g}^{-1}$) at equilibrium time, C_e is the solute concentration at equilibrium ($\mu\text{g L}^{-1}$), K_L is the Langmuir constant and q_{max} is the maximum amount of adsorbed metal ions required to form a monolayer on BC surface ($\mu\text{g g}^{-1}$), N_F is the Freundlich constant ($\mu\text{g}^{-1} (\text{g L}^{-1})^{-1/n}$) and n is the Freundlich linearity constant.

The interactions between adsorbate and adsorbent were also investigated using the Dubinin-Radushkevich, Sips and Temkin isotherm models. The first one assumes a multilayer character and it is used for distinguishing between physical and chemical adsorption of metals.⁴³⁻⁴⁵ The second model (Sips) combines Langmuir and Freundlich models and is used for predicting adsorption on heterogeneous surfaces. The last model (Temkin) assumes a uniform distribution of binding energy and it is used to check if the adsorption follows a chemisorption process.⁴⁴⁻⁴⁶

The Dubinin-Radushkevich isotherm model is calculated using the equations:^{44,47}

$$Q_e = q_m \times e^{-\beta \epsilon^2} \quad (7)$$

$$\epsilon = RT \ln(1 + 1/C_e) \quad (8)$$

$$E = 1 / \sqrt{2\beta} \quad (9)$$

where Q_e is the amount of trace metal adsorbed *per* weight of biochar ($\mu\text{g g}^{-1}$) at equilibrium; q_m is the saturation capacity; ϵ is the Polanyi potential, β is the Dubinin-Radushkevich constant, R is the gas constant ($8.31 \times 10^{-3} \text{ kJ mol}^{-1} \text{ K}^{-1}$), T is the absolute temperature and E is the mean adsorption energy.

The Sips and Temkin models are described by the following equations, respectively:^{44,48,49}

$$Q_e = q_{\text{ms}} K_s C_e^N / (1 + K_s C_e^N) \quad (10)$$

$$Q_e = (Rt / b) \ln K_T C_e \quad (11)$$

where C_e is the equilibrium concentration of adsorbate, q_{ms} is

the Sips maximum adsorption capacity, K_s is Sips equilibrium constant, N is the heterogeneity factor, b is Temkin isotherm constant, K_T is the equilibrium binding constant.

The separation factor (R_L) was calculated to verify if the adsorption is favorable to irreversibility according to Mahmoud *et al.*⁵⁰ and Bozorgi *et al.*⁵¹ (equation 12).

$$R_L = 1 / (1 + K_L \times C_0) \quad (12)$$

where C_0 represents the initial metals concentrations. According to R_L values, the adsorption is assumed to be unfavorable ($R_L > 1$), linear ($R_L = 1$), favorable ($0 < R_L < 1$), or irreversible ($R_L = 0$).

Results and Discussion

Characterization of biochar

The biochar yield on a dry mass basis decreased when the biomass was pyrolyzed at higher temperatures (500 and 600 °C) (Table S1, SI section) that was attributed to volatilization of organic matter.⁵² At the same time, the pH of BC increased probably due to the increased content of carbonates in ashes, which can be hydrolyzed, besides acid groups loss of the raw material.^{53,54}

The pyrograms (data not shown) indicated that the oxygen of biochars, produced from lignocellulosic materials, comes from a large variety of reactive functional groups, such as carboxyl, hydroxyl and carbonyl which are fragments characterized as lignin polymer.⁵⁵ Table S2 (SI section) indicates that pyrolysis products from biomass carbonization are predominant, especially in the form of hydroxyls present in phenolic functions. This data is interesting because it is known that biochars absorb/adsorb gases generated during pyrolysis.^{56,57} These adsorbed volatiles influence the adsorption behavior of other inorganic species,⁵⁸ as well as organic contaminants such as naphthalene, nitrobenzene and benzene.^{59,60} The phenolic groups found in all the analyzed samples are characterized by receiving electrons (by the Lewis model) and are associated with the electron-rich regions p in the basal planes of graphite microstructures in the biochar.⁶¹ In this way, the phenolic groups form chemical bonds with free radicals, favoring the adsorption of functional molecules in the structure of the biochar.

The analysis of Py-GC-MS was confirmed by comparison with results obtained by ¹³C NMR data. It was found a good correlation between qualitative and semi-quantitative data of the analytical techniques in relation to the chemical characteristics of the carbon formed in the BC, as also observed by Pastorova *et al.*⁶² By integrating the area of

the peaks obtained in ^{13}C NMR spectra (data not shown), the distribution of the main groups of total aromatic carbon present in the biochar samples was obtained (Figure 1). The functional groups of the BC were modified according to the increase of the pyrolysis temperature and these modifications are important to predict and investigate how their interaction with the environment in which they are inserted occurs.⁶³ This interaction is directly related to the amount of oxygen groups present on the surface of the biochar.⁶⁴

Figure 1a shows that for the BC produced from SB, the quantity and presence of the carbonyl, aromatic and alkyl groups do not occur proportionally to the increase of the pyrolysis temperature. The same behavior was observed for the portions of protonated and deprotonated carbons, as indicated in Figure 1b. Therefore, the variations of the percentages of the analyzed groups did not present a direct correlation with the increase of the pyrolysis temperature, but with the amount of pyrolytic products formed in the analytical pyrolysis (Py-GC-MS), showing that the combination of the number of organic compounds groups added to the protonated and deprotonated carbon contents is important to define the efficiency and the adsorption behavior of a biochar. This data corroborates with that reported by Bandosz,⁶⁵ who states that BC typically have amphoteric surfaces according to the variation of acidic and basic functional groups.

Adsorption of trace metals by biochars produced at different pyrolysis temperatures

The chemical and physical properties of the BC are dependent on the pyrolysis conditions. The temperature,

for instance, influences both the yield and BC nature, which will affect BC adsorption capacity.⁶⁶ The removal rates ranged from ca. 18% (minimum value recorded) for Ni^{II} using BC300 to approximately 100% for Pb^{II} using BC500 and BC600.

The trace metal removal efficiency increased when BC was produced under higher pyrolysis temperatures (Table 1). Since there was no significant difference among the BC surface functional groups, the higher porosity presented by BC400 to BC600 was responsible to the higher efficiency results. In addition, BC produced at low pyrolysis temperatures still had organic substances from the parental biomass as carbohydrates, polysaccharides, lipids and proteins, which do not contribute significantly to metal adsorption.^{36,60}

Table 1. Percentage of metal removal by biochars (after equilibrium time) produced at different pyrolysis temperatures

Metal	Removal / %			
	300 °C	400 °C	500 °C	600 °C
Cd	20.46 ± 2.66	35.00 ± 0.73	51.50 ± 0.46	36.65 ± 2.89
Cr	22.67 ± 4.18	39.63 ± 2.93	74.35 ± 0.77	67.75 ± 1.92
Cu	49.65 ± 2.08	69.16 ± 0.08	91.18 ± 0.52	95.49 ± 0.29
Ni	17.66 ± 2.04	23.12 ± 1.50	47.05 ± 1.08	41.88 ± 6.72
Pb	74.92 ± 0.08	91.10 ± 0.94	96.17 ± 0.25	92.18 ± 0.02
Zn	20.18 ± 3.51	34.90 ± 6.43	40.50 ± 2.63	47.90 ± 0.03

When all BC produced are compared, the BC500 had the best removal efficiency for most metals from a $500\ \mu\text{g L}^{-1}$ multielement solution. At these conditions, the results indicated that removal rates were Pb^{II} (96.17%) >

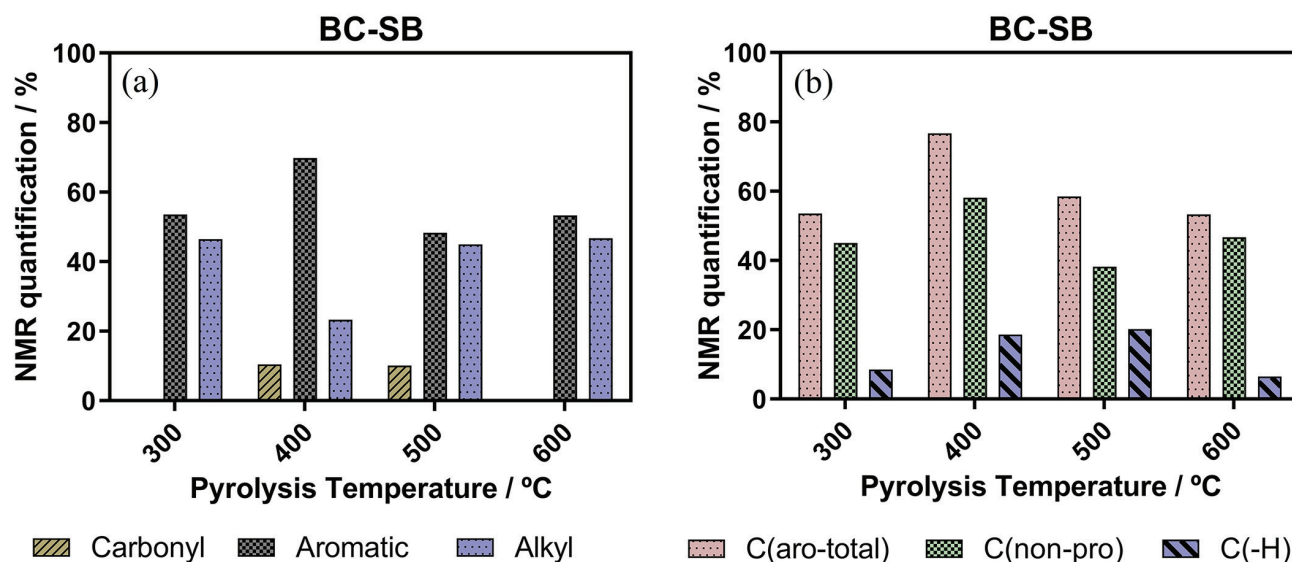


Figure 1. Analysis of carbon groups by ^{13}C NMR. (a) Determination of the portions of carbonyl, aromatic carbon and alkyl groups for biochars produced from sugarcane bagasse (BC-SB); (b) determination of the portion of protonated and deprotonated carbon.

Cu^{II} (91.18%) > Cr^{III} (74.35%) > Cd^{II} (51.50%) > Ni^{II} (47.05%) > Zn^{II} (40.50%), followed by BC600 and BC400. The trace metal with highest removal efficiency among all BC was Pb^{II} . Park *et al.*¹¹ also reported that Pb was the most adsorbed cation on sesame straw BC (produced at 700 °C) in a multielement (Cu, Cr, Cd, Pb and Zn) aqueous solution (initial pH 7). However, Cd had the lowest adsorption capacity in their investigation, different from the current study where Zn was the least adsorbed. This difference can be attributed probably to the type of organic matter used to produce the BC, the pH used in the experiments and the nature of some ions in the solution. The greater Pb^{II} sorption capacity was also observed in another study,⁶⁷ where the immobilization of the ions Cd^{II} , Cu^{II} , Ni^{II} and Pb^{II} by broiler litter-derived BC was investigated.

The structures of the original biomass were still observed in the SEM images of BC300 and BC400 (Figures S1a, S1b and S1c, SI section) when compared to other biochars (BC500 and BC600). On the other hand, changes in BC structures were observed at higher pyrolysis temperatures (> 400 °C). These changes included the increase in porosity and loss of functional groups originally present in original biomass, which can be observed in FTIR spectra (Figure 2) and can influence the removal rate of organic and inorganic contaminants in aqueous solutions.^{36,66,68}

There were no significant differences among the FTIR spectra of BC produced at different pyrolysis temperatures

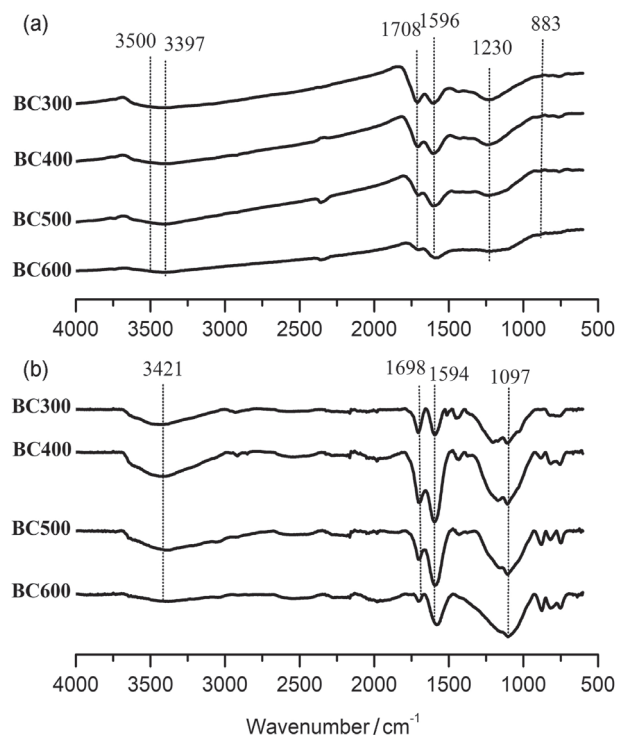


Figure 2. FTIR spectra (ATR) of biochars produced at different temperatures (a) before and (b) after interactions with metals.

(see Figure 2). In addition, the main bands present on all different BC from sugarcane bagasse are –OH stretching (3400–3500 cm^{-1}), C=O and/or C=C stretching (bands between 1708–1594 cm^{-1}) from carbonyl and carboxyl groups, C–O stretching and S compounds typical from cellulose and hemicellulose (1000–1240 cm^{-1}). At higher pyrolysis temperatures, some functional groups associated to the original biomass and hydroxyl stretching decreased noticeably (see Figure 2a, before of adsorption process).^{69,70}

After the simultaneous adsorption process of Cu^{II} , Cd^{II} , Cr^{III} , Ni^{II} , Pb^{II} and Zn^{II} ions on BC, some bands from FTIR spectra were displaced and/or disappeared. The bands at 3397, 1708 and 1596 cm^{-1} for instance shifted to 3421, 1698 and 1594 cm^{-1} , respectively; the band at 1230 cm^{-1} disappeared and the band at 1097 cm^{-1} appeared (Figure 2b). These data suggested that the functional groups on BC–OH, –C=C or C=O and –C=O were involved in the adsorption process.⁷¹

The main known adsorption mechanisms of BC are electrostatic interactions between contaminants and the adsorbent surface, cation exchange between metals on biochar surface, complexation with functional groups present at the BC surface, metal precipitation and reduction of metal species. These mechanisms for a target metal can change depending on the solution pH for instance.⁹ Considering this variability of sorption mechanisms for different target metals, the biggest challenge is to have an efficient method that removes all contaminants at the same time at different conditions. The removal of multiple contaminants by one material can represent an advantage when robust and cheap filters are required in water treatment.⁷¹

Some studies pointed out that biochar can be used to remove trace metals from wastewater. Xu *et al.*¹⁰ for instance showed that BC produced from dairy manure can be used successfully to remove Cu, Zn and Cd. The sorption was attributed to mineral components originated in the BC and surface complexation via phenolic –OH in a smaller extent. Pine and oak wood and bark BC were also tested and successfully removed Pb, Cd and As from water via ion exchange.⁷²

The adsorption, kinetics, FTIR and Py-GC-MS results and SEM micrographs suggested that the binding between the trace metals on BC500 can be attributed to surface properties of BC, as for example, their porosity and negative charges abundance due to the presence of functional groups, such as phenolic, hydroxyl and carboxyl groups. Then, chemisorption is probably the preferential adsorption mechanism and/or ionic exchange. In addition, by SEM images it is possible to notice that the mineral and carbon skeleton formed after the pyrolysis

process is maintained through the rudimentary porosity of the original material, which allows evolution of a well-defined porous structure in the pyrolyzed material. For instance, the original vegetal structure of sugarcane bagasse was imprinted on its BC and directly influenced the formation of the porous structure and, consequently, on the final adsorption behavior of biochars. As can be seen in the Figures S1b, S1c and S1d (SI section), the longitudinal section of the BC grain indicated the parenchyma tissue with many cells' spaces, which gives origin to meso and microporosity. Figure S1d showed the vessel structures from the xylem tissue, imprinting a higher porosity in the BC used in this work.

Influence of the initial concentration of trace metals on adsorption process

Since the rate between adsorbent and adsorbate can be a limiting factor in the adsorption process, this study assessed the influence of initial multielement trace metal concentration (100, 300, 500 and 700 $\mu\text{g L}^{-1}$) on the adsorption process, which was performed at 25 °C and pH 5.

The results showed that the adsorption capacity after equilibrium (q ($\mu\text{g g}^{-1}$)) was higher when initial concentrations increased. The sorption capacity for Cu^{II} on BC500 were 45.5, 151.1, 238.1, 303.9 $\mu\text{g g}^{-1}$ for the initial concentrations 100, 300, 500 and 700 $\mu\text{g L}^{-1}$, respectively. This behavior was observed to other trace metals. However, there was a clear decrease of the percentage of removal (R) when the ions concentration increased for constant mass experiments (R for 100 and 700 $\mu\text{g L}^{-1}$ multielement solutions: Cd^{II} (88 to 38%), Cr^{III} (85 to 61%), Cu^{II} (99 to 93%), Ni^{II} (85 to 35%), Pb^{II} (100 to 95%) and Zn^{II} (80 to 28%). The same trend was observed in the studies of Fan *et al.*³⁶ and Kolodyńska *et al.*³²

The decrease of R for Cd^{II} , Ni^{II} and Zn^{II} at higher trace metals concentrations can be attributed to the effective availability of adsorption sites on BC500 and the lower competition and/or preference of these ions to active sites in the presence of other ions. On the other hand, Pb^{II} and Cu^{II} took priority for active sites in all evaluated concentration.⁷³

Although there was a decrease in R for some ions at 500 $\mu\text{g L}^{-1}$ experiments, values of R were higher than 50% to all ions. Therefore, this concentration was chosen for further experiments.

Effect of adsorbent dose on adsorption

The percentage of trace metal adsorption increased when a higher BC500 dose was used (Figure 3). The removal rate increased when the mass of biochar in solution

(100 mL) increased from 0.2 g (0.4 g for Zn^{II} , which had no detectable removal at lower amounts) to 0.5 g of BC500, from 23 to 85% for Cd^{II} , 48 to 83% for Cr^{III} , 88 to 99% for Cu^{II} , 25 to 77% for Ni^{II} , 89 to 98% for Pb^{II} and 21 to 79% for Zn^{II} . This behavior was also observed by Fan *et al.*,³⁶ Ngah and Hanafiah⁷⁴ and Vaghetti *et al.*⁷⁵ and can be attributed to the higher availability of active sites on the surface of BC500 and therefore higher contact surface.

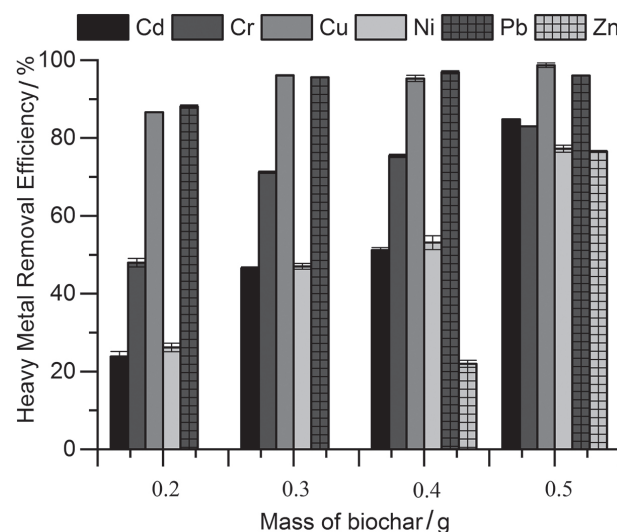


Figure 3. Percentage of metal adsorbed in the experiments using different biochar amounts.

Figure 3 shows that there is no significant increase in the percentage of Pb^{II} and Cu^{II} removed as a function of adsorbent dose. This occurs possibly because these ions are not affected by the competition of binding sites in multielement solutions.^{76,77} However, it can be assumed that Cd and Zn are more affected. Consequently, the higher the adsorbent dose, the greater the number of active sites available and the greater the adsorption of Cd and Zn ions.

Competition among different metal ions can occur affecting the adsorption of each ion present in solution. Past studies^{76,77} showed that the amount of adsorbed Cd^{II} decreases and Pb^{II} is not so much affected in multielement solutions.

Adsorption kinetics using BC500

The adsorption capacity, q ($\mu\text{g g}^{-1}$), and the removal percentage increased when the contact time increased from 0 to 1440 min between the ions Cd^{II} , Cr^{III} , Cu^{II} , Ni^{II} , Pb^{II} and Zn^{II} and BC500. The equilibrium time varied between 90 and 420 min (Figure 4), presenting the following order Pb ca. $\text{Cu} \gg \text{Cr} \gg \text{Cd} > \text{Ni} > \text{Zn}$.

The kinetics adsorption of Cu^{II} and Pb^{II} was faster when compared to the other analyzed metals since it was

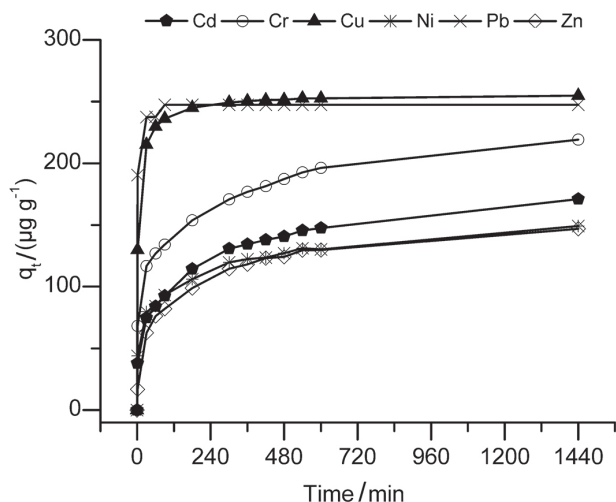


Figure 4. Influence of contact time for the adsorption process of the metals with the BC500 at 25 °C at the concentration of 500 $\mu\text{g L}^{-1}$.

necessary 90 min to approximately 90% of adsorption. The fast and high adsorption of Cu^{II} ions can be associated to hydrolysis of Cu^{II} ions at pH close to 5.5. This leads to the formation of $\text{Cu}(\text{OH})^+$ species, which are easily adsorbed. The formation of complexes among the carboxyl functional groups present on the biochar surface can also explain the Cu^{II} adsorption.⁷⁸ Other metals analyzed had a slower adsorption kinetics, since it was necessary 420 min to reach their maximum adsorption (Cd^{II} : 51.50%, Cr^{III} : 74.35%, Ni^{II} : 47.05% and Zn^{II} : 40.50%).

The adsorption kinetics of the metal ions on BC500 were evaluated using the pseudo-first and second order. The kinetic data adjusted better to second order model, which presented $1 \leq$ coefficient of determination (R^2) ≥ 0.988 and good results of chi-square (χ^2) and standard deviation (SD) (Table S3, SI section). This model describes surface adsorption and intra-particle diffusion processes controlling removal of metals by BC and suggests that chemical adsorption or ionic exchange occurred between adsorbent and adsorbate.³⁶

Adsorption isotherms

The adsorption mechanisms between adsorbent and adsorbate and the adsorption capacity of biochars can be predicted using isotherms models.⁷⁹ The adsorption isotherms of the metals analyzed on BC500 adjusted better on type L, according to Giles *et al.*⁷⁹ classification, which indicated the mass of adsorbate retained by each mass unit of adsorbent was high.⁸⁰

The adsorption isotherms of the metal ions analyzed using BC500 after 600 min of stirring are presented in the Figure 5. The concentration of metal in the equilibrium is represented by C_e ($\mu\text{g L}^{-1}$) and the adsorption capacity by

BC is represented by Q_e ($\mu\text{g g}^{-1}$). The parameters of the non-linear regression of Langmuir, Freundlich, Dubinin-Radushkevich, Sips and Temkin models are presented in Table S4 (SI section). The R_L values are essential features of the Langmuir isotherm. All values for the adsorption for the Cd, Cr, Cu, Ni and Zn ions showed a favorable adsorption isotherm and tended, consequently, to values between 0 and 1.

The isotherm that best adjusted to the data was the Freundlich due to the higher R^2 when compared to Langmuir. The Freundlich model reflects solids with heterogeneous surface and multilayer adsorption and it was probably the main adsorption mechanism of the studied species.⁸⁰

Concerning the N_F , higher values indicates a higher affinity between adsorbate and adsorbent, which means a strong interaction between metals and BC500.⁸¹ Values of $1/n$ below 1 were observed for all ions studied that also indicates favorable adsorption.³⁶

The maximum adsorption capacity in this study followed the order $\text{Cu}^{\text{II}} > \text{Cr}^{\text{III}} > \text{Cd}^{\text{II}} > \text{Ni}^{\text{II}} > \text{Zn}^{\text{II}}$ to Langmuir model and $\text{Pb}^{\text{II}} > \text{Cu}^{\text{II}} > \text{Zn}^{\text{II}} > \text{Ni}^{\text{II}} > \text{Cd}^{\text{II}} > \text{Cr}^{\text{III}}$ to Freundlich model. Park *et al.*¹¹ found similar results in experiments using sesame straw biochar, where the adsorption order to Langmuir and Freundlich were $\text{Pb} > \text{Cu} > \text{Cr} > \text{Zn} > \text{Cd}$ and $\text{Pb} > \text{Cu} > \text{Cr} > \text{Zn} > \text{Cd}$, respectively. Furthermore, the Freundlich model was the best-fit model in the experiments performed by Wang *et al.*,⁸² presenting the following adsorption order $\text{Zn} > \text{Cu} > \text{Pb}$. Ding *et al.*,³¹ using the Langmuir model, found the following order to their multielement system $\text{Pb} > \text{Cu} > \text{Zn} > \text{Ni} > \text{Cd}$. A comparison of the maximum adsorption capacities calculated by the Langmuir isotherm model for different adsorbents in literature is shown in Table S5 (SI section).

The E value of Dubinin-Radushkevich predicts the type of adsorption that occurs between adsorbate and adsorbent. If this value is $< 8 \text{ kJ mol}^{-1}$, the adsorption is physical by interactions of van der Waals. On the other hand, the adsorption is chemical if it is from 8 to 16 kJ mol^{-1} , indicating an electron transfer from adsorbent to adsorbate. Table S4 (SI section) shows that the E values calculated for all metal ions are $< 8 \text{ kJ mol}^{-1}$, suggesting that the adsorption of Cd^{II} , Pb^{II} , Cu^{II} , Cr^{III} , Ni^{II} and Zn^{II} on the surface of biochar is physical.^{83,84}

The high values of R^2 indicates that the data are also well adjusted to Sips isotherm model. When $n = 1$, this model tends to Langmuir model. On the other hand, the model takes form of Freundlich at values approaching to 0. The data (Table S4, SI section) indicates that especially the ions Cd, Ni and Zn are more associated with the Freundlich model.⁸⁵

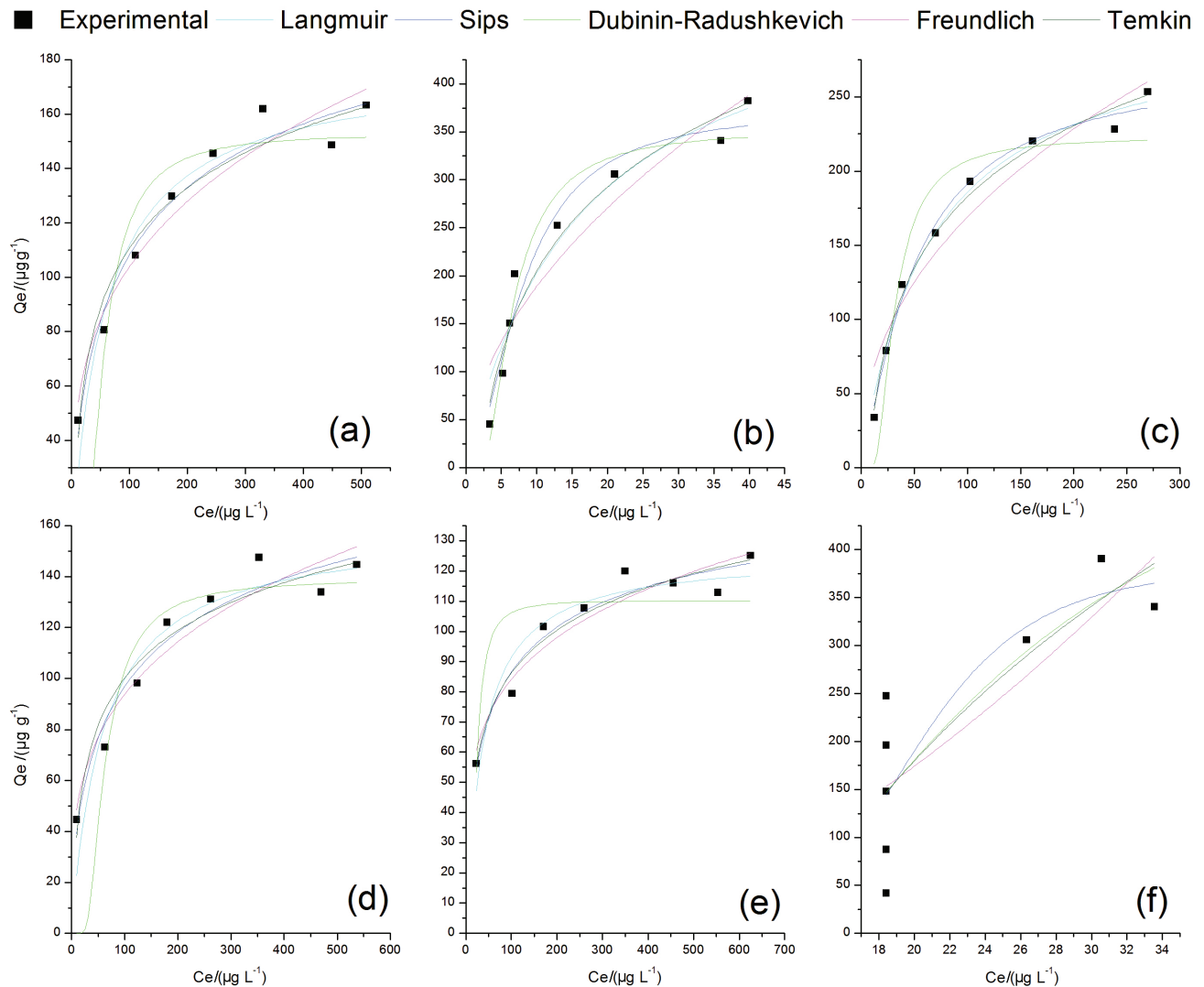


Figure 5. Theoretical isotherms and experimental data of (a) Cd^{II} , (b) Cu^{II} , (c) Cr^{III} , (d) Ni^{II} , (e) Zn^{II} and (f) Pb^{II} adsorption on BC500 at 25 °C. C_e is the solute concentration at equilibrium; Q_e is the amount of trace metal adsorbed *per* weight of biochar.

Biochar and activated carbon

Studies⁸⁶ with commercial granular activated carbon, which is a good adsorbent broadly used in remediation of trace metals from waters, aimed to compare its efficiency in removing the ions Cd^{II} , Cr^{III} , Cu^{II} , Ni^{II} , Pb^{II} and Zn^{II} using BC-SB. These tests using activated carbon were performed under same experimental conditions of the tests using BC-SB: 0.2 g of activated carbon, pH 5, and 100 mL of multielement solution ($500 \mu\text{g L}^{-1}$).

Both adsorbents activated carbon and BC500 presented similar removal rates for Pb^{II} , Cu^{II} and Cr^{III} , which ranged from 72 to 96% and were higher than removal results for Cd^{II} , Ni^{II} and Zn^{II} (52, 45 and 38%, respectively). These values were higher than the activated carbon ones, which presented removal of 25% for Cd^{II} , 23% for Ni^{II} and 15% for Zn^{II} (see Figure S3, SI section).

The adsorption process for BC-SB in the removal of Cd^{II} , Cr^{III} , Cu^{II} , Ni^{II} , Pb^{II} and Zn^{II} from multielement solutions is a promising technique, which can be used in effluents and natural waters due to easier operation and cost-benefit than activated carbon (the commercial activated carbon is expensive and the BC used in this study came from an abundant residue from agriculture in some countries such as Brazil and China).

Desorption and biochar regeneration

The desorption capacity of BC was performed to evaluate the possibility of reuse of BC since its reutilization using a diluted non-pollutant solution that does not change the BC structure is desirable. According to Kołodziejńska *et al.*³⁵ different desorbing agents such as HNO_3 , H_2SO_4 and HCl can be used for regeneration of BC. From all these agents,

the authors showed that HNO₃ (0.1 mol L⁻¹) was the most effective for desorbing trace metal ions (Cu^{II}, Zn^{II}, Co^{II}, Cd^{II} and Pb^{II}) from BC. Therefore, 0.1 mol L⁻¹ HNO₃ was used as desorbing agent in the present investigation. A higher acid concentration was not considered because it may damage the BC structure, affecting BC adsorption/desorption efficiency.³⁵

Among all adsorbed ions to BC500, Pb^{II} and Cu^{II} presented the highest desorbing capacities (D) with 89 and 80%, respectively, followed by Zn^{II} (33%), Cd^{II} (27%), Ni^{II} (24%) and Cr^{III} (6%). After the desorption process, the regenerated BC500 (with part of ions still adsorbed) was used in the second adsorption. Although the desorption was not efficient for the ions Cd^{II}, Ni^{II} and Cr^{III}, BC500 presented potential reuse capacity. The equilibrium varied between 15 and 420 min, presenting the following order Pb^{II} (100%) > Cu^{II} (99%) > Cr^{III} (78%) > Cd^{II} (54%) > Zn^{II} (40%) > Ni^{II} (47%). Similar results were recorded when BC500 was used for the first adsorption (Pb^{II} (96%) > Cu^{II} (91%) > Cr^{III} (74%) > Cd^{II} (51%) > Ni^{II} (47%) > Zn^{II} (40%)), where there was an inversion in the removal order between Zn^{II} and Ni^{II} ions and a faster adsorption kinetics of Cu^{II} and Pb^{II} compared to other metal ions (15 min to ca. 100% of adsorption).

Conclusions

Adsorption experiments using BC produced at different temperatures showed that BC500 had the highest percentage of metal removal from an aqueous solution (Cu^{II}, Cd^{II}, Cr^{III}, Ni^{II}, Pb^{II} and Zn^{II}). The removal efficiency was attributed to functional groups like carboxyl (-COOH) and hydroxyl (-OH) present in the BC structure as shown by the data obtained by Py-GC-MS, that can bind to the metal ions. Adsorption kinetics showed that the equilibrium time was 90 min to Pb^{II} and Cu^{II} and 420 min for the other metal ions analyzed. The experimental data was best adjusted to the pseudo second-order model. The isotherm analysis showed that the Freundlich and Sips models adjusted better to the experimental data.

The adsorption capacity increased following the order Pb^{II} > Cu^{II} > Cr^{III} > Cd^{II} > Ni^{II} > Zn^{II}. In addition, BC500 presented good removal results after a desorption/adsorption cycle, although the desorption was not reversible for all metal ions in solution. Therefore, the BC produced from sugarcane bagasse can act as adsorbent in the removal of metal ions from a multielement solution.

The results presented in this work demonstrated the potential of sugarcane bagasse biochar produced by slow pyrolysis as a green and low-cost adsorbent for the simultaneous removal of several contaminants

(Cu^{II}, Cd^{II}, Cr^{III}, Ni^{II}, Pb^{II} and Zn^{II}) present in an aqueous solution.

Supplementary Information

Supplementary information (scanning electron microscope images, tables and graphics) associated with this article is available free of charge at <http://jbcs.sbq.org.br> as PDF file.

Acknowledgments

The authors thank the Fundação de Amparo à Pesquisa do Estado de São Paulo (FAPESP, grant number 2016/17343-6; 2016/08215-4) for financial support and Conselho Nacional de Desenvolvimento Científico e Tecnológico (CNPq, grant number 303189/2013-4 and 158227/2018-2) and Coordenação de Aperfeiçoamento de Pessoal de Nível Superior (CAPES, PNPd) for scholarships.

Author Contributions

Adnivia S. C. Monteiro, André H. Rosa, Darllene S. Melo and Minéia A. M. de Andrade contributed to the conceptualization of the study; Adnivia S. C. Monteiro, Carolina C. Bueno, Minéia A. M. de Andrade and José I. Z. Montero performed experiments and were responsible for investigation and validation of the results; Adnivia S. C. Monteiro, Carolina C. Bueno, Erik S. J. Gontijo, João C. A. Macedo and Minéia A. M. de Andrade were responsible for data curation, formal analysis and writing original draft; André H. Rosa and Elidiane C. Rangel were responsible for reviewing and editing the manuscript; André H. Rosa was responsible for funding acquisition and resources.

References

1. Jaishankar, M.; Tseten, T.; Anbalagan, N.; Mathew, B. B.; Beeregowda, K. N.; *Interdiscip. Toxicol.* **2014**, *7*, 60.
2. Carolin, C. F.; Kumar, P. S.; Saravanan, A.; Joshiba, G. J.; Naushad, M.; *J. Environ. Chem. Eng.* **2017**, *5*, 2782.
3. Jadhav, J. P.; Kalyani, D. C.; Telke, A. A.; Phugare, S. S.; Govindwar, S. P.; *Bioresour. Technol.* **2010**, *101*, 165.
4. Tchounwou, P. B.; Yedjou, C. G.; Patlolla, A. K.; Sutton, D. J.; *Exper. Suppl.* **2012**, *101*, 133.
5. Wu, X.; Cobbina, S. J.; Mao, G.; Xu, H.; Zhang, Z.; Yang, L.; *Environ. Sci. Pollut. Res.* **2016**, *23*, 8244.
6. Fu, F.; Wang, Q.; *J. Environ. Manage.* **2011**, *92*, 407.
7. Kang, S.-Y.; Lee, J.-U.; Moon, S.-H.; Kim, K.-W.; *Chemosphere* **2004**, *56*, 141.

8. de Gisi, S.; Lofrano, G.; Grassi, M.; Notarnicola, M.; *Sustainable Mater. Technol.* **2016**, *9*, 10.
9. Li, H.; Dong, X.; da Silva, E. B.; de Oliveira, L. M.; Chen, Y.; Ma, L. Q.; *Chemosphere* **2017**, *178*, 466.
10. Xu, X.; Cao, X.; Zhao, L.; Wang, H.; Yu, H.; Gao, B.; *Environ. Sci. Pollut. Res.* **2013**, *20*, 358.
11. Park, J.-H.; Ok, Y. S.; Kim, S.-H.; Cho, J.-S.; Heo, J.-S.; Delaune, R. D.; Seo, D.-C.; *Chemosphere* **2016**, *142*, 77.
12. Nahar, K.; Chowdhury, M. A. K.; Chowdhury, M. A. H.; Rahman, A.; Mohiuddin, K. M.; *Environ. Sci. Pollut. Res.* **2018**, *25*, 7954.
13. Lyra, G. P.; dos Santos, V.; de Santis, B. C.; Rivaben, R. R.; Fischer, C.; Pallone, E. M. J. A.; Rossignolo, J. A.; *Constr. Build. Mater.* **2019**, *222*, 222.
14. Deng, W.; Van Zwieten, L.; Lin, Z.; Liu, X.; Sarmah, A. K.; Wang, H.; *J. Soils Sediments* **2017**, *17*, 632.
15. Ding, W.; Dong, X.; Ime, I. M.; Gao, B.; Ma, L. Q.; *Chemosphere* **2014**, *105*, 68.
16. Saadati, M.; Hosseini-zhad, S. J.; *Biomass Bioenergy* **2019**, *122*, 238.
17. Schlindwein, M.; Silva, L.; Vasconcelos, P.; Correa, A.; *Int. J. Adv. Soc. Sci. Humanit.* **2017**, *5*, 11.
18. Bergmann, J. C.; Trichez, D.; Sallet, L. P.; e Silva, F. C. P.; Almeida, J. R. M. In *Advances in Sugarcane Biorefinery*; Chandel, A. K.; Silveira, M. H. L., eds.; Elsevier: Amsterdam, 2018, ch. 4.
19. Martínez-Fernández, D.; Vítková, M.; Michálková, Z.; Komárek, M. In *Phytoremediation: Management of Environmental Contaminants*, vol. 5; Ansari, A. A.; Gill, S. S.; Gill, R.; Lanza, G. R.; Newman, L., eds.; Springer International Publishing: Cham, 2017, p. 369-403.
20. Liganiso, L.; Buthelezi, T.; Tshwafo, M.; *Wood Res.* **2019**, *6*, 273.
21. Pachón, E. R.; Vaskan, P.; Gorgens, J. F.; Gnansounou, E. In *Refining Biomass Residues for Sustainable Energy and Bioproducts*; Kumar, R. P.; Gnansounou, E.; Raman, J. K.; Baskar, G., eds.; Academic Press: Oxford, 2020, p. 567-597.
22. Verma, D.; Gope, P. C.; Maheshwari, M. K.; Sharma, R. K.; *J. Mater. Environ. Sci.* **2012**, *3*, 1079.
23. Milani, P. A.; Consonni, J. L.; Labuto, G.; Carrilho, E. N. V. M.; *Environ. Sci. Pollut. Res.* **2018**, *25*, 35906.
24. Guilherme, A. A.; Dantas, P. V. F.; Santos, E. S.; Fernandes, F. A. N.; Macedo, G. R.; *Braz. J. Chem. Eng.* **2015**, *32*, 23.
25. Kaal, J.; Martínez Cortizas, A.; Reyes, O.; Soliño, M.; *J. Anal. Appl. Pyrolysis* **2012**, *95*, 205.
26. Fabbri, D.; Torri, C.; Spokas, K. A.; *J. Anal. Appl. Pyrolysis* **2012**, *93*, 77.
27. Stevenson, F. J.; *Humus Chemistry: Genesis, Composition and Reactions*, 2nd ed.; John Wiley & Sons: New York, 1994.
28. Galán, J.; Rodríguez, A.; Gómez, J. M.; Allen, S. J.; Walker, G. M.; *Chem. Eng. J. (Amsterdam, Neth.)* **2013**, *219*, 62.
29. Saka, C.; Şahin, Ö.; Küçük, M. M.; *Int. J. Environ. Sci. Technol.* **2012**, *9*, 379.
30. Kołodyńska, D.; Wnętrzak, R.; Leahy, J. J.; Hayes, M. H. B.; Kwapiński, W.; Hubicki, Z.; *Chem. Eng. J. (Amsterdam, Neth.)* **2012**, *197*, 295.
31. Ding, Z.; Hu, X.; Wan, Y.; Wang, S.; Gao, B.; *J. Ind. Eng. Chem. (Amsterdam, Neth.)* **2016**, *33*, 239.
32. Kołodyńska, D.; Bak, J.; Koziol, M.; Pylychuk, L. V.; *Nanoscale Res. Lett.* **2017**, *12*, 433.
33. Ding, Y.; Liu, Y.; Liu, S.; Li, Z.; Tan, X.; Huang, X.; Zeng, G.; Zhou, Y.; Zheng, B.; Cai, X.; *RSC Adv.* **2016**, *6*, 5223.
34. Park, J.-H.; Cho, J.-S.; Ok, Y. S.; Kim, S.-H.; Heo, J.-S.; Delaune, R. D.; Seo, D.-C.; *Arch. Agron. Soil Sci.* **2016**, *62*, 617.
35. Kołodyńska, D.; Krukowska, J.; Thomas, P.; *Chem. Eng. J. (Amsterdam, Neth.)* **2017**, *307*, 353.
36. Fan, S.; Li, H.; Wang, Y.; Wang, Z.; Tang, J.; Tang, J.; Li, X.; *Res. Chem. Intermed.* **2018**, *44*, 135.
37. Ho, Y. S.; McKay, G.; *Process Biochem. (Oxford, U. K.)* **1999**, *34*, 451.
38. Moussout, H.; Ahlafi, H.; Aazza, M.; Maghat, H.; *Karbala Int. J. Mod. Sci.* **2018**, *4*, 244.
39. Lagergren, S.; *K. Sven. Vetenskapsakad. Handl.* **1898**, *24*, 1.
40. Agrafioti, E.; Kalderis, D.; Diamadopoulos, E.; *J. Environ. Manage.* **2014**, *146*, 444.
41. Langmuir, I.; *J. Am. Chem. Soc.* **1918**, *40*, 1361.
42. Freundlich, H. M. F.; *J. Phys. Chem.* **1906**, *57*, 385.
43. Bhatnagar, A.; Kumar, E.; Sillanpää, M.; *Chem. Eng. J. (Amsterdam, Neth.)* **2010**, *163*, 317.
44. Saruchi; Kumar, V.; *Arabian J. Chem.* **2019**, *12*, 316.
45. Ayawei, N.; Ebelegi, A. N.; Wankasi, D.; *J. Chem.* **2017**, *2017*, 11.
46. Foo, K. Y.; Hameed, B. H.; *Chem. Eng. J.* **2010**, *156*, 2.
47. Dubinin, M.; Radushkevich, L.; *Dokl. Akad. Nauk SSSR* **1947**, *55*, 331.
48. Tempkin, M. J.; Pyzhev, V.; *Acta Physicochim. URSS* **1940**, *12*, 217.
49. Sips, R.; *J. Chem. Phys.* **1948**, *16*, 490.
50. Mahmoud, M. E.; El Zokm, G. M.; Farag, A. E. M.; Abdelwahab, M. S.; *Environ. Sci. Pollut. Res.* **2017**, *24*, 18218.
51. Bozorgi, M.; Abbasizadeh, S.; Samani, F.; Mousavi, S. E.; *Environ. Sci. Pollut. Res.* **2018**, *25*, 17457.
52. Demirbas, A.; *J. Anal. Appl. Pyrolysis* **2004**, *72*, 243.
53. Mimmo, T.; Buono, D. D.; Terzano, R.; Tomasi, N.; Vigani, G.; Crecchio, C.; Pinton, R.; Zocchi, G.; Cesco, S.; *Eur. J. Soil Science* **2014**, *65*, 629.
54. Yuan, J.-H.; Xu, R.-K.; Zhang, H.; *Bioresour. Technol.* **2011**, *102*, 3488.
55. Duman, G.; Okutucu, C.; Ucar, S.; Stahl, R.; Yanik, J.; *Bioresour. Technol.* **2011**, *102*, 1869.
56. Chouchene, A.; Jeguirim, M.; Khiari, B.; Trouvé, G.; Zagrouba, F.; *J. Anal. Appl. Pyrolysis* **2010**, *87*, 168.

57. Song, J.; Peng, P.; *J. Anal. Appl. Pyrolysis* **2010**, *87*, 129.
58. Uchimiya, M.; Wartelle, L. H.; Klasson, K. T.; Fortier, C. A.; Lima, I. M.; *J. Agric. Food Chem.* **2011**, *59*, 2501.
59. Cheng, C.-H.; Lehmann, J.; Engelhard, M. H.; *Geochim. Cosmochim. Acta* **2008**, *72*, 1598.
60. Chun, Y.; Sheng, G.; Chiou, C. T.; Xing, B.; *Environ. Sci. Technol.* **2004**, *38*, 4649.
61. Brennan, J. K.; Bandoz, T. J.; Thomson, K.; Gubbins, K. E.; *Colloids Surf., A* **2001**, *187*, 539.
62. Pastorova, I.; Botto, R. E.; Arisz, P. W.; Boon, J. J.; *Carbohydr. Res.* **1994**, *262*, 27.
63. Preston, C. M.; Schmidt, M. W. I.; *Biogeosciences* **2006**, *3*, 397.
64. Boehm, H. P.; *Carbon* **1994**, *32*, 759.
65. Bandosz, T. J.; *Activated Carbon Surfaces in Environmental Remediation*, 1st ed.; Elsevier Science: Oxford, 2006.
66. Chen, T.; Zhang, Y.; Wang, H.; Lu, W.; Zhou, Z.; Zhang, Y.; Ren, L.; *Bioresour. Technol.* **2014**, *164*, 47.
67. Uchimiya, M.; Lima, I. M.; Klasson, K. T.; Chang, S.; Wartelle, L. H.; Rodgers, J. E.; *J. Agric. Food Chem.* **2010**, *58*, 5538.
68. Chen, C.-P.; Cheng, C.-H.; Huang, Y.-H.; Chen, C.-T.; Lai, C.-M.; Menyailo, O. V.; Fan, L.-J.; Yang, Y.-W.; *Geoderma* **2014**, *232*, 581.
69. Sun, H.; Hockaday, W. C.; Masiello, C. A.; Zygourakis, K.; *Ind. Eng. Chem. Res.* **2012**, *51*, 3587.
70. Hossain, M. K.; Strezov, V.; Chan, K. Y.; Ziolkowski, A.; Nelson, P. F.; *J. Environ. Manage.* **2011**, *92*, 223.
71. Herrmann, S.; de Matteis, L.; de la Fuente, J. M.; Mitchell, S. G.; Streb, C.; *Angew. Chem., Int. Ed.* **2017**, *56*, 1667.
72. Mohan, D.; Pittman, C. U.; Bricka, M.; Smith, F.; Yancey, B.; Mohammad, J.; Steele, P. H.; Alexandre-Franco, M. F.; Gómez-Serrano, V.; Gong, H.; *J. Colloid Interface Sci.* **2007**, *310*, 57.
73. Vilvanathan, S.; Shanthakumar, S.; *Process Saf. Environ. Prot.* **2015**, *96*, 98.
74. Ngah, W. S. W.; Hanafiah, M. A. K. M.; *Bioresour. Technol.* **2008**, *99*, 3935.
75. Vaghetti, J. C. P.; Lima, E. C.; Royer, B.; da Cunha, B. M.; Cardoso, N. F.; Brasil, J. L.; Dias, S. L. P.; *J. Hazard. Mater.* **2009**, *162*, 270.
76. Ahmad, M.; Rajapaksha, A. U.; Lim, J. E.; Zhang, M.; Bolan, N.; Mohan, D.; Vithanage, M.; Lee, S. S.; Ok, Y. S.; *Chemosphere* **2014**, *99*, 19.
77. Wang, Y.; Liu, R. H.; *Fuel Process. Technol.* **2017**, *160*, 55.
78. Jin, H.; Hanif, M. U.; Capareda, S.; Chang, Z.; Huang, H.; Ai, Y.; *J. Environ. Chem. Eng.* **2016**, *4*, 365.
79. Giles, C. H.; Smith, D.; Huitson, A.; *J. Colloid Interface Sci.* **1974**, *47*, 755.
80. Nascimento, R. F.; Lima, A. C. A.; Vidal, C. B.; Melo, D. Q.; Raulino, G. S. C.; *Adsorção: Aspectos Teóricos e Aplicações Ambientais*; Imprensa Universitária: Fortaleza, 2014.
81. Site, A. D.; *J. Phys. Chem. Ref. Data* **2001**, *30*, 187.
82. Wang, Y.-Y.; Liu, Y.-X.; Lu, H.-H.; Yang, R.-Q.; Yang, S.-M.; *J. Solid State Chem.* **2018**, *261*, 53.
83. Hu, Q.; Zhang, Z.; *J. Mol. Liq.* **2019**, *277*, 646.
84. Shafiee, M.; Abedi, M. A.; Abbaszadeh, S.; Sheshdeh, R. K.; Mousavi, S. E.; Shohani, S.; *Sep. Sci. Technol. (Philadelphia, PA, U. S.)* **2019**, DOI: 10.1080/01496395.2019.1624572.
85. Kumara, N. T. R. N.; Hamdan, N.; Petra, M. I.; Tennakoon, K. U.; Ekanayake, P.; *J. Chem.* **2014**, *2014*, 6.
86. Deng, B.; Caviness, M.; Gu, Z. In *ACS Symposium Series*, vol. 915; O'Day, P. A.; Vlassopoulos, D.; Meng, X.; Benning, L. G., eds.; American Chemical Society: Washington, DC, 2005, p. 284-293.

Submitted: October 23, 2019

Published online: March 11, 2020

